CONCRETE LIBRARY OF JSCE NO. 12. MARCH 1989

ANALYTICAL MODEL FOR RC PANEL ELEMENTS SUBJECTED TO IN-PLANE FORCES

(Translation from Concrete Journal of JCI, Vol.25, No.9, Sept., 1987)

Junich IZUMO

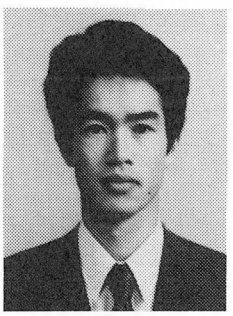

Hiroshi SHIMA

Hajime OKAMURA

SYNOPSIS

The constitutive law for a RC panel element has been developed by combining the existing constitutive laws for cracked concrete and the new constitutive law for yielded steel in RC, all of which have been obtained by uniaxial loading tests of RC elements. In this study, the constitutive law for yielded steel has been introduced on the assumption that a stress distribution of yielded steel between cracks is represented by a cosine function. Further, the proposed constitutive law for the RC panel element has been verified through the experiments of the RC panel element conducted by Collins & Vecchio and Aoyagi & Yamada. It has been confirmed that the proposed model for the RC panel element can accurately describe the behavior of the RC panel element subjected to in-plane stresses and be applicable to FEM.

J. Izumo is a assistant professor of civil engineering at the University of Kanto Gakuin, Yokohama, Japan. He received his Doctor of Engineering from the University of Tokyo in 1988. His research interests include non-linear analyses of RC members and structures. He is a member of JSCE and JCI.

H. Shima is a assistant professor of civil engineering at the University of Tokushima, Tokushima, Japan. He received his Doctor of Engineering from the University of Tokyo in 1987. His research interests include seismic design of RC members and structures. He is a member of JSCE, JCI, JSMS and ACI.

H. Okamura is a professor of civil engineering at the University of Tokyo, Tokyo, Japan. His research interests include fatigue and shear of RC members, durability design of RC structures and application of FEM to RC. He is a member of JSCE, JCI, IABSE and a fellow of ACI.

NOTATION

The following symbols are used in this paper

$\{\sigma_c\}$:stress vector of concrete relating to the local coordinate system
$\{\sigma'_c\}$:stress vector of concrete relating to the global coordinate system
$\{\sigma_s\}$:stress vector of steel relating to the local coordinate system
$\{\sigma'_s\}$:stress vector of steel relating to the global coordinate system
$\{\varepsilon_c\}$:strain vector of concrete relating to the local coordinate system
$\{\varepsilon_s\}$:strain vector of steel relating to the local coordinate system
$\{\varepsilon\}$:strain vector of the RC panel relating to the global coordinate system
$[D_c]$:stiffness matrix of concrete
$[D_s]$:stiffness matrix of steel.
$[D_{RC}]$:stiffness matrix of the RC panel element
E_s :stiffness of steel
E_{sh} :strain hardening ratio
E_0 :initial tangential modulus of uncracked concrete
E_c :Young's modulus of concrete
E_{cr} :compressive stiffness of cracked concrete
G_{cr} :shear stiffness of cracked concrete.
G_0 :shear stiffness of uncracked concrete
G_1 :shear stiffness of cracked concrete given by $G_1=36/\varepsilon_t$
p_x :steel ratio in x-direction
p_y :steel ratio in y-direction
σ_1, σ_2:principal stress of concrete ($\sigma_1 \geqq \sigma_2$)
σ_t :tensile stress of concrete in the direction perpendicular to the cracked face
σ_c :compressive stress in the direction perpendicular to the cracked face
σ_s :steel stress at the cracked face
$\overline{\sigma}_s$:mean stress of steel
σ_x :normal stress of the RC panel element which acts on the plane; BC
σ_y :normal stress of the RC panel element which acts on the plane; AC
τ_{xy} :shear stress of the RC panel element which acts on the plane; AC, BC
τ :shear stress which acts along the cracked face
σ_{sx} :steel stress in x'-direction (refer to Fig.1-1)
σ_{sy} :steel stress in y'-direction (refer to Fig.1-1)
f_t :tensile strength of concrete under uniaxial stress
f_{tb} :tensile strength of concrete under biaxial stresses
f'_c :cylinder strength of concrete.
ε_{cr} :tensile strain at cracking
ε_p :plastic strain given by the Maekawa model
ε_t :tensile strain in the direction perpendicular to the cracked face
$\overline{\varepsilon}_s$:mean strain of steel
ε_{sh} :strain when strain hardening starts
ε_{s0} :mean strain of steel at the former load step
f_y :yield strength of steel.
f_u :tensile strength of steel
K_1, K_2 :coefficient given by Appendix II
K_c :fracture parameter of cracked concrete ($=\omega K$)
K :fracture parameter of uncracked concrete
A_{sx} :cross-sectional area of steel in x'-direction

A_{sy} :cross-sectional area of steel in y'-direction
A :stress amplitude of steel
A_o :stress amplitude of steel at the former load step
θ :angle created by the cracked face and the global coordinate system
α :angle created by the steel axle and the global coordinate system
ν_c :Poisson's ratio of concrete.
c :parameter which express bond characteristics.
t :panel thickness

1. INTRODUCTION

Finite Element Method (FEM) has been used in analyzing reinforced concrete (RC) structures. This is not only due to the advancement of computer technology but due to the advantage of treating complex loading and complicated boundary conditions with the integrated analytical method. There are three schools in applying FEM to RC from micro-level to macro-level[1]. In the school of micro-level, phenomena such as the bond mechanism, the shear transfer mechanism at the cracking interface and the cracking progress; are accurately developed into a model to understand the true behavior of RC. On the other hand, the macro-level school analyzes the behavior of full-scale structures and this school attempts to use the analytical results directly for structural design.

There is an another school between these two schools, which pursues the relationship between load and displacement on RC members subjected to in-plane stresses such as shear walls. In these RC members, usually, a number of steel bars are placed and also smeared cracks shall appear. Taking advantage of these characteristics, the behavior of RC members subjected to in-plane stresses can be traced with an efficient accuracy by using the smeared crack model. When an analytical model for RC members and/or structures subjected to in-plane stresses is developed and efficient for wide range application, data necessary for design may be obtained through calculations without performing experiments. Such as studies[2][3][4][5][6] follow this school.

This study also follows the third school. The purpose of this study is to develop the constitutive law for a RC panel element subjected to in-plane stresses. In the authors' laboratory, the constitutive laws for cracked concrete[3][5][6] have been intensively studied while making contacts with Dr. Aoyagi and Dr. Yamada. Further, based on these studies, the authors have developed the constitutive law for the RC panel elements subjected to in-plane stresses by combining the existing constitutive law for cracked concrete and for steel. However, the proposed constitutive law has been derived from the experiment results under uniaxial stress condition. Therefore, the application of each constitutive law should be evaluated through a comparison with the test results of the RC panels element under biaxial stress condition. Further the proposed constitutive law for the RC panel element should be also verified.

2. DEVELOPMENT METHOD OF THE CONSTITUTIVE LAW FOR THE RC PANEL ELEMENT

2.1 Premise Conditions

Methods for handling cracks in the analysis may be categorized into a discrete crack model and a smeared crack model. The first method installs so-called the link element which represents the discontinuity of concrete between cracks. The cracking direction cannot be obtained directly through this method, though it is effective for analyzing RC members like beams and/or columns, in which one crack affects the behavior of RC members. The latter method treats cracked concrete as a continuous body. In this method, the development or the progress of cracks are not as important as the general behavior of cracked RC members at a microscopic view. Therefore, this method is effective for analyzing RC members like shear walls or membrane RC members. As a RC panel element subjected to in-plane stresses are analyzing objects, the smeared crack model has been adopted in this study. Therefore, the stresses and the strains on the RC panel element mean the average stresses and the average strains respectively.

The constitutive law for the RC panel element has been made up of the existing constitutive laws for cracked concrete and steel under uniaxial stress condition. As there are existing constitutive laws obtained from the experiments, the constitutive law for the RC panel element is easier to be constructed when these existing constitutive laws are combined. The tension stiffening model, the compressive stiffness model of cracked concrete and steel model after yielding developed in the authors' laboratory and the shear stiffness model of cracked concrete proposed by Aoyagi and Yamada have been introduced to the constitutive law for the RC panel element.

In developing the constitutive law for the RC panel element, monotonic proportional loading and non-proportional loading have been taken into consideration. However, the proposed constitutive law can not be applied to the RC panel element subjected to cyclic loading. The authors are planning to extend the constitutive law presented in this study to the constitutive law that can apply to any loading hysteresis.

2. 2 Formulation of the Constitutive Law for the RC Panel Element

The stresses of the RC panel element can be represented by superposition of the stresses of cracked concrete and the stresses of steel. The stresses of concrete and steel are respectively expressed by;

$$\{\sigma_c\}=[D_c]\{\varepsilon_c\} \tag{1}$$

$$\{\sigma_s\}=[D_s]\{\varepsilon_s\} \tag{2}$$

In this study, the engineering shear strain is used for the shear strain. The stiffness matrix of concrete after cracking is orthogonal anisotropy matrix. The coordinate system prepared for stiffness matrix are different between concrete and steel. The stiffness matrix of concrete is taken with respect to the local coordinate system composed of the axis paralleling to the cracked face and the axis crossing the cracked face. On the other hand, the stiffness matrix of steel is taken with respect to the local coordinate system coinciding with the steel axes. By using the transformation matrix, the stresses and the strains related

to the local coordinate system can be respectively transformed to the stresses and the strains related to the global coordinate system. Therefore, eq.(1) and eq.(2) can be changed to eq.(3) and eq.(4).

$$\{\sigma'_c\}=[T(\theta)]^t[D_c][T(\theta)]\{\varepsilon\} \tag{3}$$

$$\{\sigma'_s\}=[T(\alpha)]^t[D_s][T(\alpha)]\{\varepsilon\} \tag{4}$$

$[T(\theta)]$ indicates the transformation matrix and is expressed by;

$$[T(\theta)]=\begin{bmatrix} \cos^2\theta & \sin^2\theta & \cos\theta\sin\theta \\ \sin^2\theta & \cos^2\theta & -\cos\theta\sin\theta \\ -2\cos\theta\sin\theta & 2\cos\theta\sin\theta & \cos^2\theta-\sin^2\theta \end{bmatrix} \tag{5}$$

The stresses of the RC panel element are expressed by summation of the stresses of concrete and steel.

$$\{\sigma'_{RC}\}=\{\sigma'_c\}+\{\sigma'_s\}=[D_{RC}]\{\varepsilon\} \tag{6}$$

where $[D_{RC}]$ indicates the stiffness matrix of the RC panel element and is expressed by eq.(7).

$$[D_{RC}]=[T(\theta)]^t[D_c][T(\theta)]+[T(\alpha)]^t[D_s][T(\alpha)] \tag{7}$$

Eq.(6) can also be changed into the incremental form, as eq.(8).

$$\{d\sigma'_{RC}\}=\{d\sigma'_c\}+\{d\sigma'_s\}=[D_{RC}]\{d\varepsilon\} \tag{8}$$

In this case, the stiffness matrix $[D_{RC}]$ indicates the tangential stiffness. The constitutive law for the RC panel element can be formulated by the constitutive laws for concrete and steel. It must be emphasized that the constitutive laws for concrete and steel in RC are different from those for concrete and steel as a simple material. The RC panel element is considered elastic until cracks appear. Therefore, before cracking, the constitutive laws for concrete and steel as a single material can be used for the constitutive law for the RC panel element. As bond action and dowel action shall occur after cracking, these phenomena must be considered in developing the constitutive law for the RC panel element. For stiffness matrix of concrete, eq.(9) is used before cracking and eq.(10) for after cracking.

$$[D_c]=\frac{E_c}{1-\nu_c^2}\begin{bmatrix} 1 & \nu_c & 0 \\ \nu_c & 1 & 0 \\ 0 & 0 & (1-\nu_c)/2 \end{bmatrix} \tag{9}$$

$$[D_c]=\begin{bmatrix} 0 & 0 & 0 \\ 0 & E_{cr} & 0 \\ 0 & 0 & G_{cr} \end{bmatrix} \tag{10}$$

The stiffness matrix of the RC panel element is used to solve eq.(8) for the

given stress increment. The value of tensile stiffness becomes negative when using the stiffness matrix in the incremental form. Therefore, in the analysis of the RC panel element, convergence after cracking becomes very instable. In order to obtain the stable solution, zero has been substituted for the negative value of the tensile stiffness. The stiffness matrix of steel is expressed by eq.(11). Assumed that steel only resists in the direction along the bars, the shear stiffness of steel is quite smaller than the shear stiffness of concrete.

$$[D_c]=\begin{bmatrix} p_x E_s & 0 & 0 \\ 0 & p_y E_s & 0 \\ 0 & 0 & 0 \end{bmatrix} \tag{11}$$

After yielding, the stiffness of steel is given by the proposed constitutive law presented in the chapter 4.

2.3 Analytical Method

The analytical method follows the flow chart (see Fig.1). The analysis is done by solving the eq.(6) for the given external stresses of the RC panel element. The following is calculating procedure.

[Calculating Procedure]

1) Give the incremental stresses $\{d\sigma'_{RC}\}$ that act on the RC panel element.
2) Obtain total stress $\{\sigma'_{RC}\}$.
3) Solve the eq.(8) to obtain the incremental strains $\{d\varepsilon\}$.
4) Obtain the total strains $\{\varepsilon\}$ by the calculated incremental strain $\{\varepsilon\}$.
5) Obtain the strains $\{\varepsilon_c\}$ and $\{\varepsilon_s\}$ in the local coordinate system of concrete and steel by using the transformation matrix.
6) Obtain the stresses $\{\sigma_c\}_{cal}$ and $\{\sigma_s\}_{cal}$ through the constitutive law for concrete and steel.
7) Transform the obtained stresses $\{\sigma_c\}_{cal}$ and $\{\sigma_s\}_{cal}$ to the stresses relating to the global coordinate system and obtain the RC panel element stresses $\{\sigma'_{RC}\}_{cal}$
8) Repeat the calculation till the difference between the stresses $\{\sigma'_{RC}\}_{cal}$ and the given external stresses $\{\sigma'_{RC}\}$ is within the error variation range.
9) Repeat the loop of 3) to 8), if convergence is not obtained.

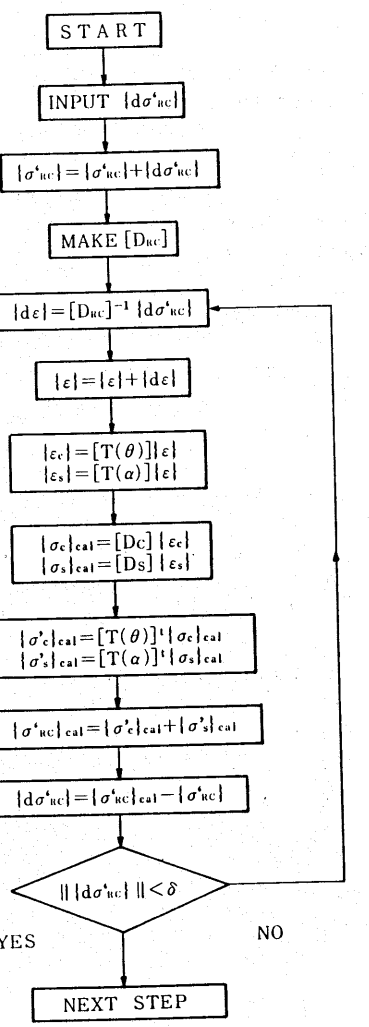

Fig.1 Flow chart

2.4 Verification Method of the Proposed Constitutive Law

The proposed constitutive law for the RC panel element is composed of the constitutive law for cracked concrete and steel. Each constitutive law is developed by the experimental results of the RC elements under uniaxial stress field. Therefore, the proposed constitutive law must be verified through the experiments of the the RC panel element subjected to biaixal stresses. Okamura and Maekawa[7] have already reported the sensibilities of each constitutive law to the behavior of the RC panel element. Based on their study, the applications of each constitutive law to the RC panel element are investigated. Each constitutive law has been verified through the analysis of the test data which are greatly effected by each constitutive law. The authors also have verified the constitutive law for the RC panel element by the test data which are effected by all of the constitutive laws. Further, the total evaluation of the proposed constitutive law has been performed.

Table 1 Test Specimen

	Specimen	Load[1]	p_x	p_y/p_x	α (degree)	f_y (MPa)	f'_c (MPa)	f_{t1}[2] (MPa)	f_{t2}[3] (MPa)	f_{t2}/f_{t1}	
	PV3	PS	0.48	1.00	0	662	26.6	2.39	1.68	0.70	
	PV4	PS	1.06	1.00	0	242	26.6	2.39	1.68	0.80	
	PV9	PS	1.79	1.00	0	455	11.6	1.37	1.91	1.39	
	PV10	PS	1.79	0.56	0	276	14.5	1.60	1.29	0.81	
	PV11	PS	1.79	0.73	0	235	15.6	1.68	1.60	0.95	
	PV12	PS	1.79	0.25	0	469	16.0	1.71	1.67	1.00	
	PV16	PS	0.74	1.00	0	255	21.7	2.09	1.71	0.94	
	PV18	PS	1.79	0.18	0	431	19.5	1.95	1.96	1.00	
Collins·	PV19	PS	1.79	0.40	0	x:458	19.0	1.91	1.95	1.08	average
Vecchio						y:299					1.11
Test	PV20	PS	1.79	0.50	0	x:460	19.6	1.95	2.07	1.14	
						y:297					coefficient
	PV21	PS	1.79	0.73	0	x:458	19.5	1.95	2.54	1.30	of variation
						y:302					20.9%
	PV22	PS	1.79	0.85	0	x:458	19.6	1.95	2.54	1.30	
						y:420					
	PV23	SBC	1.79	1.00	0	518	20.5	2.01	2.81	1.40	
	PV25	SBC	1.79	1.00	0	466	19.2	1.93	2.70	1.40	
	PV27	PS	1.79	1.00	0	442	20.5	2.01	2.81	1.40	
	PV28	SBT	1.79	1.00	0	483	19.0	1.91	2.29	1.20	
	PV29	SBC	1.79	0.57	0	x:441	21.7	2.09	2.09	1.00	
						y:324					
	No.7	UT	0.71	1.00	22.5	371	23.4	2.21	1.76	0.80	average
Aoyagi·	No.11	UT	0.71	1.00	12.5	371	20.3	2.00	1.44	0.72	0.77
Yamada	No.13	UT	0.71	1.00	22.5	371	21.1	2.05	1.71	0.83	coefficient
Test	No.23	CT	1.18	1.00	22.5	371	19.8	1.97	1.60	0.81	of variation
	No.24	UT	1.18	0.50	22.5	371	21.3	2.07	1.45	0.70	7.5%

1) PS:Pure Shear, SBT:Shear and Biaxial Tension, SBC:Shear and Biaxial Compression, UT:Uniaxial Tension, CT:Principal Compression and Principal Tension

2) $f_{t1}=0.583f'^{2/3}_c$

3) Tensile strength coincided with the test results

The test data conducted by Collins & Vecchio[2] and Aoyagi & Yamada[8] have been used to verify the proposed constitutive model. As uniform stress fields are formed in these experiments, the test data may be easily analyzed through one element. The specimens with a failure at the end of the RC panel element, the specimens with pre-set cracks and the specimens that break right after the appearance of cracks, have been removed from the Collins·Vecchio experiments. The specimens that generate cracks along the steel bars and the specimens with pre-set cracks also have been removed from the Aoyagi·Yamada experiments. Table 1 shows the conditions of the specimens.

3. CRITERIA OF CRACKING AND ANGLE OF CRACKING

3.1 Criteria of Cracking

Cracks occur when principal tensile strain reaches the tensile limit strain of concrete. It is assumed that the tensile stress shall be kept constant from the point where the principal tensile stress reaches the tensile strength to the point where cracks occur. The value from 0.01% to 0.03% is usually used for the tensile limit strain. The tensile limit strain is generally larger than the strain reaching the tensile strength of concrete. This is because concrete is considered to be kept plastic from the strain at reaching the tensile strength to the tensile limit strain. Considering the flexural strength of concrete being roughly double the value of tensile strength, the doubled value of tensile strain corresponding to the tensile strength is adopted for the value of the tensile limit strain (see Fig.2).

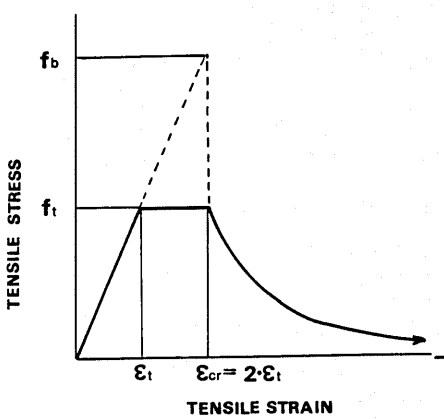

Fig.2 The relationship between tensile strength and tensile limit strain

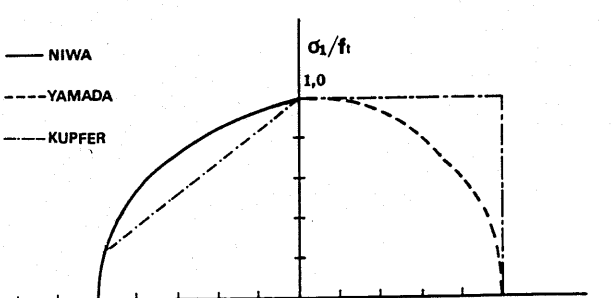

Fig.3 Tension failure criteria of concrete under biaxial stresses

Kupfer[9] studied the failure criteria of concrete under biaxial stresses. In his study, the accuracy for compressive failure is high. However the accuracy for tensile failure is not sufficient. Therefore, the formula presented by Niwa et al. studying the compression-tension range of concrete[10] and the formula presented by Yamada et al. studying the tension-tension range[8] will be used for this study (see Fig.3). Maekawa clarified that the loading path does not affect the failure criteria when it is a monotonic loading[11]. These formulas;

eq.(12) can be used for the tensile failure of concrete regardless of the loading path.

$$f_{tb}/f_t=\sqrt[3]{1-(\sigma_2/f'_c)} \quad \text{for } \sigma_2 \leqq 0 \quad \text{(Formula by Niwa et al.[10])} \qquad (12)$$
$$f_{tb}/f_t=1-0.3(\sigma_2/\sigma_1)^2 \quad \text{for } \sigma_2 > 0 \quad \text{(Formula by Yamada et al.[8])}$$

The tensile strength of concrete affects not only the criteria of cracking but also tension stiffening. Therefore, the tensile strength must be estimated accurately. When the cracking load is defined by the load when the stiffness of the RC panel element rapidly changes in the load-displacement relationship, the calculated principal tensile stresses at the cracking load are shown in Table 1. Table 1 also shows the tensile stress ratio of the tensile strength obtained from compressive strength to the calculated tensile stresses at the cracking load. For the Collins·Vecchio experiments and the Aoyagi·Yamada experiments, each average ratio is 1.11 and 0.77. and each coefficient of variation is 20.9% and 7.5%. Dispersion for the Collins·Vecchio experiments is wide. This is the reason that concrete mixtures and the curing condition of each specimen were different. As the tensile strength affects the behavior of the RC panel element after cracking, the tensile strength which gives the same cracking load with test results are adopted to verify the proposed model.

3.2 Angle of Cracking

The angle of cracking affects the direction in which tension stiffening acts and the shear stress transmitted through the cracked face. The authors assume that the cracking direction is perpendicular to the direction in which the principal tensile stress acts. On the other hand, Yamada et al.[8] have expressed the cracking angle with a linear function of principal tensile stress ratio for the tension-tension range of concrete from their experimental results. Although, the cracking angle in the tension-tension range is affected by a shape of a specimen and placement of steel bars. For example, in case of the cylindrical container subjected to internal forces[12], cracks occurred in arbitrary radial directions at the upper circular slab. It is difficult to define the cracking direction for the tension-tension range of concrete. This is because cracks generate in every possible directions. Therefore, the cracking angle is always set perpendicular to the direction along the principal tensile stress acts. In this study, reversed cyclic loading is not considered. Cracks are considered to generate in one direction and does not change the direction even if the direction of the principal stress changes.

4. CONSTITUTIVE MODEL FOR TENSION STIFFENING

4.1 Tension Stiffening Model

The bond action exists between steel and concrete even after cracking. Therefore, concrete bears the tensile stress between cracks and in consequence the stiffness of the RC panel element is higher than that of steel itself. There are two method to treat this phenomenon. The first method is to modifying the stiffness of steel. The second one is to give the tensile stress to concrete even after cracking. A study by Gilbert & Warner[13] is related to the first

method. Studies relating to the second method are CEB-FIP model code[14], Morita & Kaku[15], Yoshikawa & Tanabe[16], Gilbert & Warner[13] and Milford & Schonbrich[17]. In CEB-FIP model code, the mean stress-mean strain relationship of cracked concrete which is a function of steel stress is used. Yoshikawa expresses tension stiffening in terms of a reinforcement ratio function. Morita ·Kaku model, Gilbert·Warner model and Milford·Schnobrich model are characterized by having no relationship with steel and being expressed by the unique mean stress-mean strain relationship. These models are useful because they can give the tensile stress of concrete in any direction regardless of the steel axis. The authors will adopt Okamura·Maekawa model for tension stiffening[7], which is given by the eq.(13). The parameter c is introduced in the eq.(13) so as to be taken the bond effect into consideration.

$$\sigma_t/f_t=(\varepsilon_{cr}/\varepsilon_t)^c \qquad (13)$$

The tensile stress of concrete is given by eq.(13) in the direction orthogonal to the cracked face. Generally, the direction, in which tensile stress of concrete is given, is different from the direction of steel bars under biaxial stress condition. Further, Okamura·Maekawa model provides the tensile stress of concrete indifferent to a reinforcement ratio. Therefore, it is necessary to verify this presented model with the RC panel tests under in-plane stresses condition.

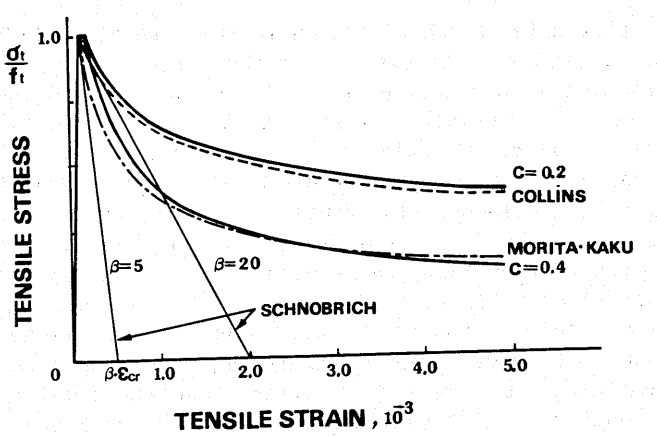

Fig.4 Tension stiffening model

Fig.4 shows the Okamura·Maekawa model, the Collins·Vecchio model[2] and the Morita·Kaku model. The Okamura·Maekawa model with parameter c=0.2 shows the same curve obtained from the Collins·Vecchio model. On the other hand, the Okamura·Maekawa model with parameter c=0.4 show the same curve obtained from the Morita·Kaku model. The Collins·Vecchio model evaluate tension stiffening higher than other models. This is because the steel mesh, that shows different bond nature to a deformed bar, is used in the Collins·Vecchio experiments. The parameter c=0.2 is introduced for the Collins·Vecchio experiments and c=0.4 for the RC panel experiments that use deformed bars.

4.2 Constitutive Model for Steel after Yielding

(1) Criterion of yielding

The tensile stiffness as RC is expressed by superposition of the stiffness of concrete and steel. Until now, the analysis for RC has been performed on the assumption that yielding starts when the mean strain of the RC element reaches the yield strain of steel. However, the stress acting along the steel bar between cracks is not unique because of bond action. The steel stress becomes into maximum at the cracked face where concrete does not bear the tensile stress. Therefore, the tensile stiffness of the RC element results in higher values, when the yield criterion of the RC element is evaluated through the mean strain of steel. This phenomenon can be confirmed through the uniaxial tension experiments of the RC element performed by Tamai et al.[6]. The yielding of the RC element starts when the steel stress at the cracked face reaches the yielding stress. This is described by;

$$\sigma_s = f_y \tag{14}$$

The the principal tensile stress direction of concrete and that of steel do not always conform with each other. Therefore, the steel stresses acting on the RC panel element are more difficult to be obtained when compared to the RC element under uniaxial tensile stress condition. Solving the equilibrium relating to the global coordinate system, while considering of the triangular Free Body containing the cracked face, the steel stresses at the cracked face can be obtained (refer to Appendix I).

(2) Constitutive Model for steel after yielding

The stiffness of yielded steel in RC depends on the mean stress of steel when yielding starts. The strain hardening rate has the tendency to increase when the mean stress of steel at yielding is lower (the strain hardening rate describes the hardening of the mean stress-mean strain relationship in RC and it is different from the strain hardening rate of steel as a simple material). When steel is yielded in the low stress condition, the plastic area of steel is rather small. Therefore, the stiffness of steel in RC is higher than that of steel yielded in the high stress condition. The authors have adopted a cosine function as a stress distribution of steel after yielding and well succeeded to describe the behavior of the RC element by this function[6]. The eq.(15) is the generalized constitutive law for steel after yielding obtained by introducing the cosine function as the stress distribution of steel after yielding.

$$\overline{\sigma}_s = K_1(\overline{\varepsilon}_s - K_2) \tag{15}$$

The tensile stress of the RC panel element uses eq.(13) for tension stiffening and eq.(15) for steel after yielding. As the bond deterioration occurs after yielding, tension stiffening is smaller than one obtained from eq.(15). However, the effect of tension stiffening after yielding is considered to be small. Therefore, this effect is neglected.

4.3 Verification of the Tension Stiffening Model

The tension stiffening model has been obtained from the uniaxial tension test of the RC elements. The adopted tension stiffening model may not be applicable to the the RC panel element subjected to in-plane stresses. Therefore, verification of the tension stiffening model must be needed through a comparison with the experimental data of the the RC panel element. Following points will be studied for verification.

1) Will the behavior of the RC panel element be described, when eq.(13) is being used as the constitutive law for tension stiffening ?
2) Is the Okamura·Maekawa model applicable to the RC panel element in case of the direction of steel being different from that of the principal tensile stress of concrete ?
3) Will the criterion of yielding and the constitutive law for steel after yielding describe the behavior of the RC panel element ?

The analyses for verification have been done through selected specimens that are effected by tension stiffening in the Collins·Vecchio experiments and the Aoyagi·Yamada experiments. Specimens selected from the Collins·Vecchio experiments are PV3, PV9 and PV28, which are not effected by the shear stiffness because of the bars arrangement being isotropic. Effects of the compressive stiffness is relatively small except for the neighborhood of failure because the acting stresses are relatively low. Further, the steel does not yield, so these specimens are suitable for verification of the tension stiffening model. The specimens PV3 and PV9 are subjected to pure shear stress. The specimen PV28 is subjected to pure shear stress and tensile stresses in x and y directions. Fig.5 shows analytical results. The shear strain of the RC panel element and steel strains in x and y directions agree well with the experimental results, when the analyses are performed with the parameter c set to 0.2. It can be recognized that the adopted tension stiffening model describes well the tension stiffening behavior of the RC panel element.

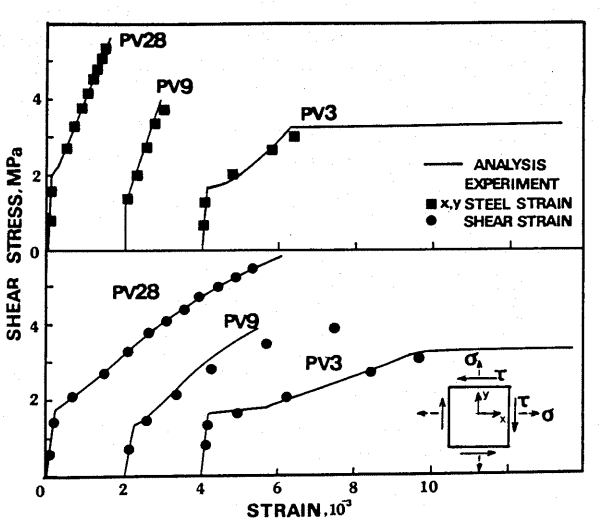

Fig.5 Analytical results (verification for tension stiffening model)

The stress acted on the specimen PV4 is low and the placement of reinforcing bars is isotropic. In this case, reinforcing bars yield in the both directions. Fig.6 shows the analytical results. Fig.6 also shows the analytical results assuming that yielding occurs when the mean strain of steel reaches the yielding strain of steel. When the tensile stresses of concrete and steel are simply added as the tensile stress of the RC panel element, the yield point of RC will be evaluated in high value and will effect the behavior of the RC panel element after yielding. On the other hand, the presented constitutive law for steel accurately evaluates the lowering of stiffness caused by yielding at the cracked face.

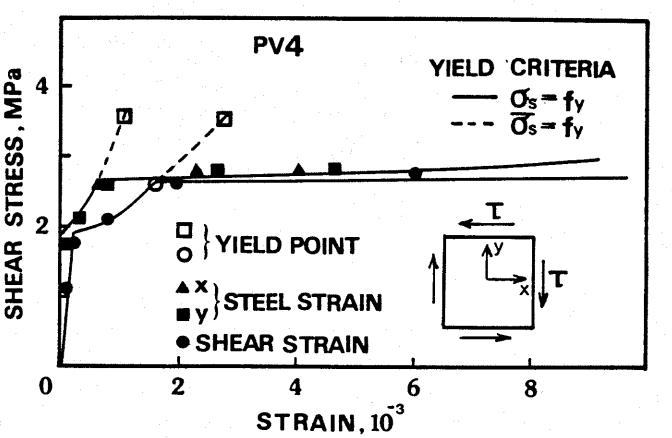

Fig.6 Analytical results (verification for constitutive law for steel)

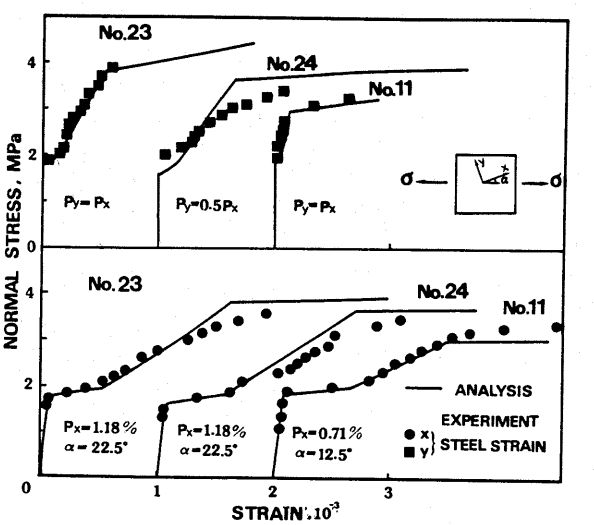

Fig.7 Analytical results (verification for tension stiffening model)

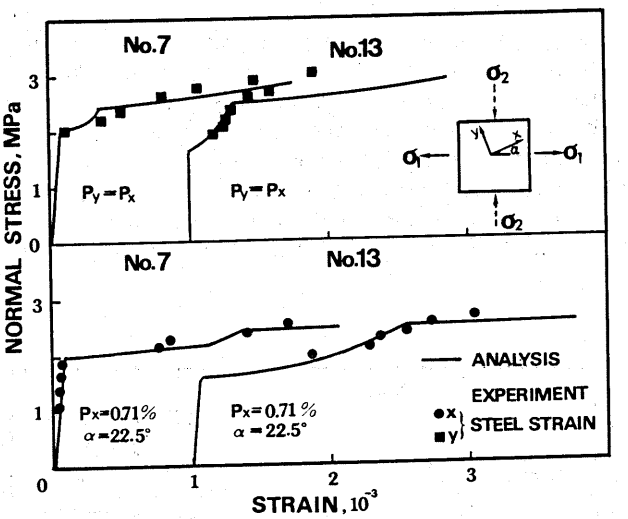

Fig.8 Analytical results (verification for tension stiffening model)

Table 2 shows the observed values and the analytical values regarding to the shear strain and the maximum shear stress. The maximum shear stress ratio of the observed value to the analytical value is 0.94 in average. The shear stress ratio of the observed value to the analytical value for each shear strain; 0.1%, 0.2% and 0.4% is 0.98 in average. These averages are consistent to the analytical results. Table 3, Fig.7 and Fig.8 show the analytical results for the Aoyagi·Yamada experiments. The loading condition of the chosen specimens are in the uniaxial tension state (Except specimen No.13 is the in tension-compression biaxial loading state). However, the direction of the principal tensile stress of concrete and the direction of the tensile stress of steel are different. These specimens can be used to study the application of the presented tension stiffening model to the the RC panel element. Table 3 shows the observed value and the analytical value of yield stress and the maximum stress. The observed strain of steel in the Aoyagi·Yamada experiments does not have efficient accuracy after yielding, therefore, the behavior after yielding can not be followed. The analytical value and observed value have good correspondence before yielding. The analyzed yield stresses are slightly higher than the observed values and slightly lower for the maximum stresses. However, the observed values and the analytical values have good correspondence. The direction of steel axis and that of the principal tensile stress of concrete are different in specimen No.7 and No.11. From these analytical results, the tension stiffening model can be applied to the in-plane stress field even when directions of the principal tensile stress of concrete and the steel stress are different each other.

Table 2 Analytical results (Collins·Vecchio experiments)

Specimen	Maximum Shear stress (MPa) (1)	(2)	(1)/(2)	Average	Shear Strain ($\times 10^{-3}$)	Shear Stress (MPa) (1)	(2)	(1)/(2)	Average
PV3	3.07	3.41	0.90	0.94	1.00	1.52	1.67	0.91	0.98
					2.00	1.96	1.86	1.05	
PV4	2.89	3.06	0.94		1.00	2.06	2.16	0.95	
					2.00	2.65	2.65	1.00	
					4.00	2.74	2.65	1.03	
PV9	3.74	4.00	0.94		1.00	1.81	1.96	0.92	
					2.00	2.60	2.99	0.87	
PV28	5.80	6.02	0.96		1.00	2.25	2.30	0.98	
					2.00	3.23	3.14	1.03	
					4.00	4.85	4.70	1.03	
PV23	8.87	7.97	1.11	1.03	1.00	4.51	4.51	1.00	1.00
					2.00	5.78	5.78	1.00	
					4.00	7.55	7.64	0.98	
PV25	9.12	8.67	1.05		1.00	5.78	6.08	0.95	
					2.00	7.30	7.55	0.97	
PV27	6.35	6.76	0.94		1.00	3.33	3.23	1.03	
					2.00	4.36	4.21	1.03	
					4.00	5.98	5.98	1.00	
PV12	3.13	3.18	0.98	0.94	1.00	1.96	1.86	1.05	1.05
					2.00	2.35	2.16	1.09	
					4.00	2.84	2.70	1.05	
PV18	3.04	3.26	0.93		1.00	2.16	2.06	1.05	
					2.00	2.50	2.25	1.11	
					4.00	2.74	2.84	0.96	
PV20	4.26	4.52	0.94		1.00	2.74	2.60	1.05	
					2.00	3.23	3.09	1.05	
					4.00	4.02	3.63	1.11	
PV21	5.03	5.68	0.89		1.00	2.94	2.84	1.04	
					2.00	3.72	3.72	1.00	
					4.00	4.66	4.51	1.03	
PV10	3.97	4.12	0.96	0.93	1.00	2.01	2.06	0.98	1.02
					2.00	2.70	2.84	0.95	
					4.00	3.68	3.53	1.04	
PV11	3.56	4.05	0.88		1.00	2.16	2.21	0.98	
					2.00	2.94	3.14	0.94	
PV16	2.14	2.32	0.92		1.00	2.01	2.16	0.93	
					1.00	2.40	2.35	1.02	
PV19	3.95	4.09	0.97		2.00	3.04	2.65	1.15	
					4.00	3.53	3.23	1.09	
PV22	6.07	6.24	0.97		1.00	3.04	2.94	1.03	
					2.00	4.02	3.92	1.03	
					4.00	5.68	5.59	1.02	
PV29	5.80	6.47	0.90		1.00	2.55	2.45	1.04	
					2.00	3.23	3.14	1.03	
					4.00	3.97	3.72	1.07	
Total Evaluation				Average 0.95 Coefficient of Variation 6.0%					Average 1.01 Coeffcient of Variation 5.6%

(1) Experiment (2) Analysis

Table 3 Analytical results (Aoyagi·Yamada experiments)

Specimen	Yield Stress (MPa) (1)	(2)	(1)/(2)	Maximum Stress (MPa) (1)	(2)	(1)/(2)
No.7	2.35	2.45	0.96	3.26	2.92	1.12
No.11	2.87	2.94	0.98	3.66	3.33	1.10
No.13	2.48	2.50	0.99	3.01	2.97	1.01
No.23	3.46	3.82	0.91	5.13	4.53	1.13
No.24	3.33	3.63	0.92	4.24	4.02	1.05
	Average Coefficient of Variation		0.95 3.7%		Average Coefficient of Variation	1.08 4.7%

5. CONSTITUTIVE MODEL FOR COMPRESSIVE CRACKED CONCRETE

5.1 Constitutive Model for Compressive Cracked Concrete

Collins and Vecchio tested the the RC panel element subjected to biaxial stresses. They reported that the compressive stiffness of concrete paralleling to the cracked face was reduced[2]. Maekawa proposed an idea that the lowering stiffness of concrete was due to the stress relaxation in the vicinity of cracks. He also presented the constitutive law for compressive cracked concrete, introducing the elasto-plastic fracture model for plain concrete to cracked concrete[3]. Miyahara et al.[5] have conducted uniaxial compression tests of the RC element with pre-set cracks paralleling to the loading axis. The lowering strength of cracked concrete has been confirmed to be represented by the tensile strain in the direction orthogonal to the cracked face. Furthermore, they have reported that the compressive strength only lowers 0.65 to the compressive strength of uncracked concrete. Primarily, the Maekawa model is introduced to this study to represent the lowering stiffness of cracked concrete. The stiffness lowering initial point and stiffness lowering end point will be decided through the Collins·Vecchio experiments.

From the Collins·Vecchio experiments, the specimens PV23, PV25 and PV27 have been selected. These specimens are much effected by the lowering compressive stiffness. From these testing results, compressive stresses in the direction paralleling to the cracked face are obtained. The obtained compressive stresses are normalized through compressive stresses, which are obtained from the Maekawa model for uncracked concrete. Fig.9 shows the relationship between normalized compressive stresses and the tensile strain obtained from the Collins·Vecchio experiments, the Maekawa model[3], the proposed model which modifies Maekawa model and the model proposed by Collins and Vecchio[18]. In the modified Maekawa model, the initial point of the lowering stiffness and the end point of the lowering stiffness are decided through the test results conducted by Collins and Vecchio. There are correlations between the lowering of compressive stiffness and tensile strain in the direction orthogonal to the cracked face.

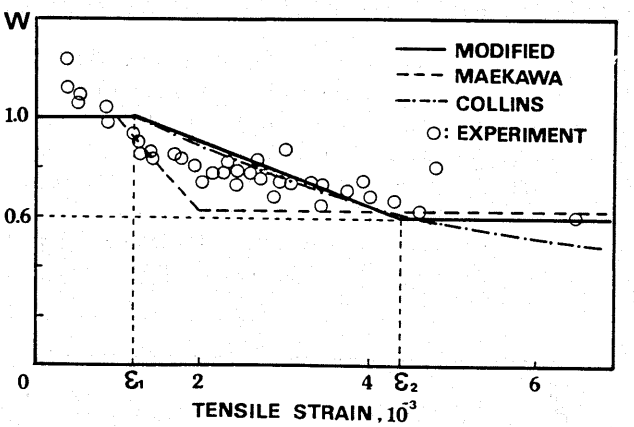

Fig.9 Relationship between the the lowering rate of concrete strength and the average tensile strain perpendicular to the cracked face

The authors describe the constitutive law for compressive cracked concrete by eq.(16).

$$\sigma_c = E_0 K_c (\varepsilon_c - \varepsilon_p) \tag{16}$$

The fracture parameter of cracked concrete K_c is given by $K_0 \omega$, where K_0 denotes the fracture parameter of uncracked concrete obtained from the Maekawa model and ω denotes the reducing factor. ω is expressed by the following equation as a function of the tensile strain in the direction orthogonal to the cracked face.

$$\omega = 1.0 \qquad \text{for } \varepsilon_t \leqq \varepsilon_1$$
$$\omega = 1.0 - 0.4(\varepsilon_t - \varepsilon_1)/(\varepsilon_2 - \varepsilon_1) \qquad \text{for } \varepsilon_t \leqq \varepsilon_2$$
$$\omega = 0.6 \qquad \text{for } \varepsilon_t > \varepsilon_2$$

where, $\varepsilon_1 = 0.0012$ and $\varepsilon_2 = 0.0044$

Considering all of the specimens fractured by compression, Collins & Vecchio arranged the test data and introduced the model that explained the stiffness lowering of compressive cracked concrete. In their model, the compressive strength of cracked concrete becomes closer to zero as the tensile strain increases. Taking the experimental results conducted by Miyahara et al.[5] into consideration, the authors keep the lowering of the concrete strength up to 0.6.

In this study, the cylinder strength is being used as the compressive strength for the analyses. The compressive strength is generally lower than the cylinder strength that is affected by confinement through friction of the loading surface. The cylinder strength in the Collins·Vecchio experiments was approximately 20 MPa. The effects of confinement through friction are considered to be small. However, there is a report that the compressive strength drops near to 0.9, when the cylinder strength is over 50 MPa[19]. The cylinder strength, being used as a compressive strength, must be reduced, when the concrete strength is high.

5.2 Verification of the Constitutive Model for Compressive Cracked Concrete

Fig.10 shows the analytical results of PV23, PV25 and PV27 obtained through the presented constitutive law. The specimen PV27 is subjected to pure shear stress. The specimens PV23 and PV25 are subjected to shear stress and compressive stresses in x and y directions. Table 2 shows the observed values and the analytical values regarding to the shear strain and the maximum shear stress. Analytical results describe the behavior of the RC panel element very well. This is because the proposed constitutive law are introduced from the Collins·Vecchio experiments. This constitutive law will be used in the analyses of the RC panel element hereafter.

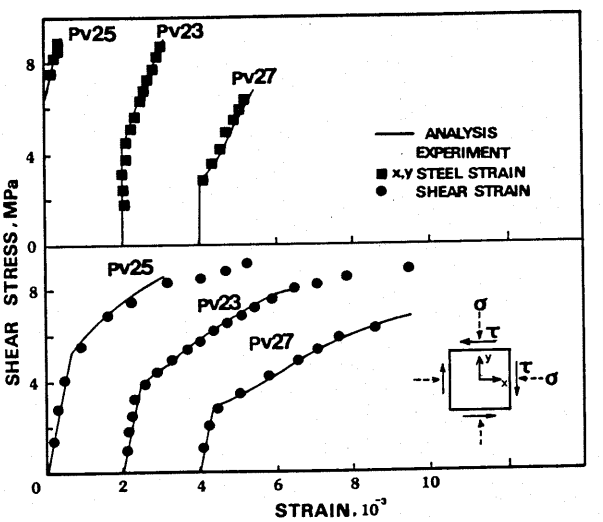

Fig.10 Analytical results (verification for the modified Maekawa model)

6. CONSTITUTIVE MODEL FOR SHEAR DEFORMATION ALONG CRACK

6.1 Constitutive Model for Shear Deformation along Crack

There are existing constitutive laws for shear deformation along crack studied by Aoyagi & Yamada[4], Cervenka[20], Fardis[21], Fenwick[22] and Walraven[23]. Assumption of the crack width and the crack spacing are necessary for all of the constitutive laws except the Aoyagi·Yamada model and the Cervenka model. Further, the dowel action must be studied. The Aoyagi·Yamada model and the Cervenka model were developed in order to apply to the the RC panel element with smeared cracks. These models describe the shear stiffness transmitted by cracks as the function of the principal tensile strain. Therefore, these models are useful for analyzing the the RC panel element.

The Cervenka model does not consider the crack spacing and another parameter must be set to describe the shear stiffness. The Aoyagi·Yamada model can represent the shear stiffness with one valued function of the tensile strain. Therefore, the Aoyagi·Yamada model has been adopted for the shear stiffness of

cracked concrete in this study. It will be described by eq.(17) and is equivalent to the shear stiffness that are connected in series with the shear stiffness represented by Aoyagi & Yamada and the shear stiffness between cracks (refer to Fig.11).

$$G_{cr}=1/(1/G_O+1/G_1) \tag{17}$$

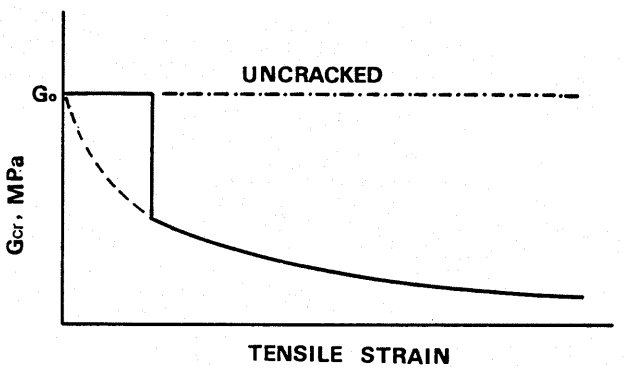

Fig.11 Model for shear stiffness of cracked concrete

6.2 Verification of the Constitutive Model for Shear Deformation

The specimens PV12, PV18, PV20 and PV21 have been chosen from the Collins·Vecchio experiments to verify the presented constitutive law. These specimens are subjected to pure shear stress. As steel bars are placed anisotropically in these specimens, the selected specimens are affected by the shear stiffness. Further, the steel in these specimen shall be yielded. Before verifying the constitutive law for shear deformation, the effect of steel yielding should be studied. Using the specimen PV12 that has strong anisotropy, the sensibility analysis has been performed by changing the strain hardening rate of steel or the shear stiffness. As the strain hardening rate of steel cannot be obtained from the Collins·Vecchio experiments data, it is given by eq.(18). Eq.(18) sets the strain at reaching the tensile strength of steel to 10% and keeps the strain hardening rate constant from yielding to breaking. The strain that starts hardening of steel has been assumed to 1.5% considering the specification of standard reinforcement in Japan.

$$E_{sh}=10(f_u-f_y) \tag{18}$$

Fig.12(a) shows the analytical result in case of changing the strain hardening rate from 1/2 times to 2 times of the strain hardening rate given by eq.(18) and in case of no yield plateau. The difference obtained by changing the strain hardening rate and the yield plateau are small enough to be neglected. When the shear stiffness is changed to 2/3 times and 1 times of the shear stiffness given by eq.(17), the effect of changing the shear stiffness is bigger than the changing the strain hardening rate of steel (see Fig.12(b)). In case of PV12,

the behavior is affected more by the shear stiffness than the tensile stiffness of yielded steel. The same results have been obtained from PV18, PV20 and PV21. Therefore, these specimen may be used for verifying the shear stiffness model.

Fig.12 and Fig.13 show the analytical results of PV12, PV18, PV20 and PV21. The analytical results fit all behaviors of each experiment results. Table 2 show the observed values and the analytical values regarding to the shear strain and the maximum shear stress. The maximum shear stress ratio of the observed value to the analytical value is 0.94 in average. The shear stress ratio of the observed value to the analytical value for each shear strain; 0.1%, 0.2% and 0.4% is 1.05 in average. The model presented by Aoyagi & Yamada sufficiently shows the shear behavior of the RC panel element.

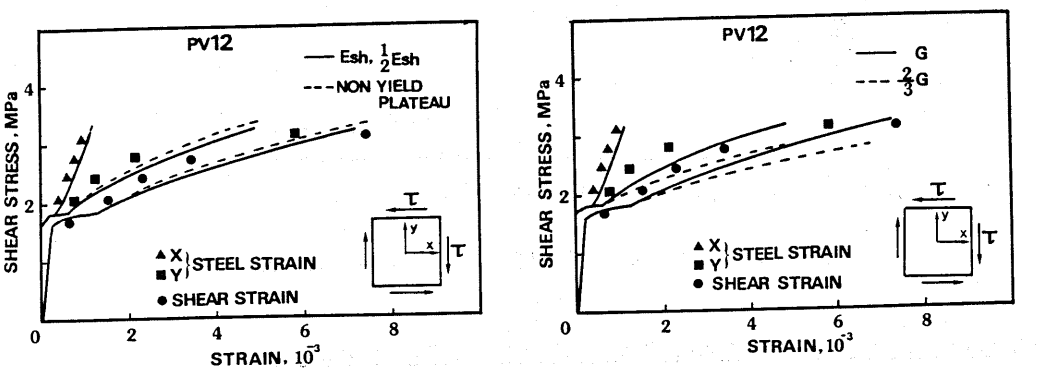

(a) effect of tensile stiffness for steel (b) effect of shear stiffness

Fig.12 Sensibility analysis

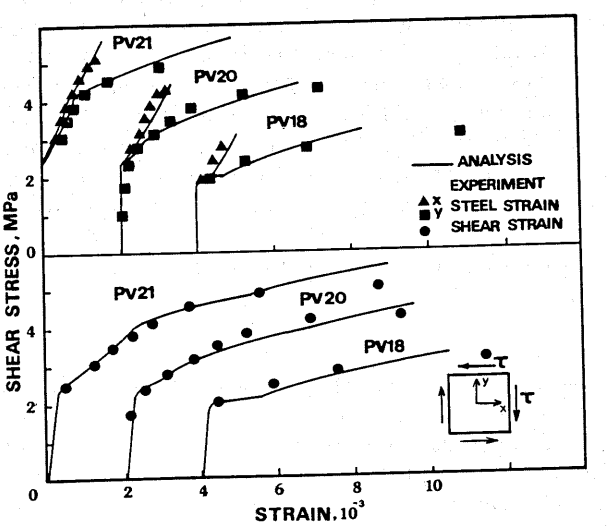

Fig. 13 Analytical results (verification for shear stffness model)

The Collins·Vecchio experiments used to verify the constitutive law for shear had relatively low cylinder strength of concrete, which were approximately 20MPa. Therefore, the effect of the concrete strength influencing on the shear stiffness is small. Although, when the concrete strength is relatively high, the effect of the concrete strength on the shear stiffness must be considered. The verification of the shear stiffness model for the RC panel element which have the high strength of concrete, is also necessary but there is not any satisfactory experimental data for verification at this present.

7. TOTAL EVALUATION

From the analytical results in aforesaid chapters, the proposed constitutive law describe the behavior of tension stiffening, compressive cracked concrete and shear deformation in the RC panel element. In addition to those analytical results, six more specimens have been analyzed by using the proposed constitutive model. The analytical results are shown in Fig.14 and Fig.15. Results sufficiently describe the behavior of the RC panel element.

Analytical results concerning the maximum shear stresses and deformations are described in Table 2. The maximum stress ratio of the observed value to the analytical value is 0.93 in average. The shear stress ratio of the observed value to the analytical value for each shear strain;0.1%, 0.2% and 0.4% is 1.02 in average. Further, regarding all of analytical results, the maximum stress ratio is 0.95 in average and 6.0% for coefficient of variation and the shear stress ratio is 1.02 in average and 5.6% for coefficient of variation. The proposed constitutive law can be applied to the RC panel element subjected to in-plane stresses.

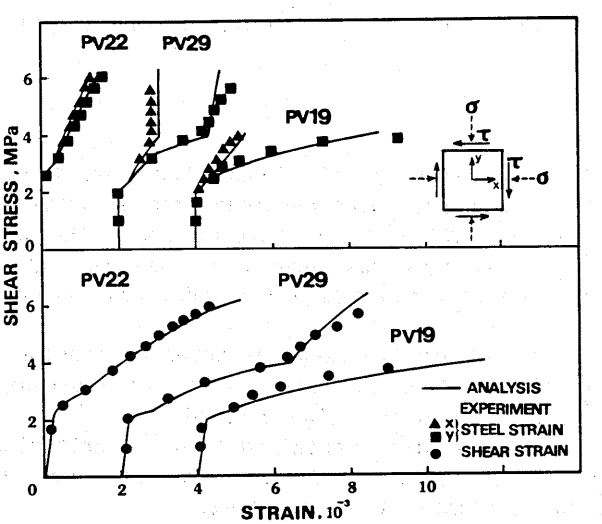

Fig.14 Analytical results (verification for the RC panel element)

In this study, the analyses have been done by using the tensile strength of concrete being coincided with the observed cracking load. The study by Shioya et al.[24] reports that the scale effect is being confirmed in the tensile strength. Further, the tensile strength is much effected by the drying shrinkage. The tensile strength greatly affects the behavior of RC after cracking. An accurate estimation of these affects are the subject for future studies.

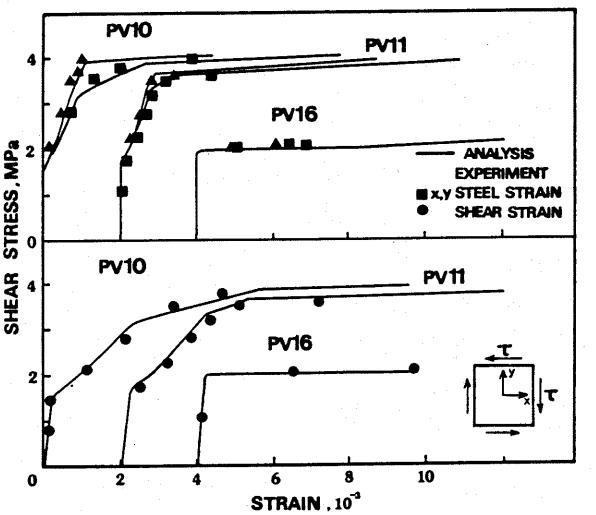

Fig.15 Analytical results (verification for the RC panel element)

8. CONCLUSIONS

The constitutive law for the RC panel element has been developed by combining the constitutive laws which have been obtained from uniaxial testing results of the RC elements. The application of the proposed law to the the RC panel element subjected to in-plane stresses has been confirmed through the test results conducted by Collins & Vecchio and Aoyagi & Yamada. Conclusions are as follows.

(1) The behavior of the RC panel element affected by tension stiffening can be represented by the Okamura·Maekawa model, which is expressed by the tensile strain in the direction orthogonal to the cracked face.
(2) The constitutive law for steel, obtained from the criterion of yielding and the assumption of the steel stress distribution can accurately describe the behavior of the RC panel element after yielding.
(3) The modified Maekawa model, reducing the compressive stiffness with the tensile strain in the direction orthogonal to the cracked face, can represent the compressive behavior of the RC panel element.
(4) The Aoyagi·Yamada model, expressed by the tensile strain in the direction

orthogonal to the cracked face, can sufficiently represent the shear behavior of the RC panel element.
(5) The constitutive law for the RC panel element, developed by the constitutive laws for cracked concrete and for steel after yielding, can accurately predict the deformation and the ultimate strength of the RC panel element in the range of experiments used in this verification.

Following points must be considered when applying the constructed constitutive law for the RC panel element.
(1) The tensile strength, which decides the crack generating condition and the post crack behavior of RC, is influenced by the scale effect and the drying shrinkage. Therefore, the tensile strength must be obtained with an accuracy.
(2) The cylinder strength being used for the compressive strength, the effect of confinement through friction on the cylinder surface should be taken into consideration in case of the high strength of concrete.
(3) The concrete strength must be considered for the shear stiffness, when concrete strength is high.

ACKNOWLEDGEMENTS

The authors express their deep appreciation to Dr. Kouichi MAEKAWA, associate professor of the University of Tokyo, with the development of the analytical program; Mr. Shinichi TAMAI with experiments; and Dr. Sivasubramaiam former graduate student of the University of Tokyo with the analyses. The authors are grateful to Dr. Yamada for the usage of the valuable experiment data. This study was carried out under Grant-in-Aids for scientific researches No. 60302062 from Ministry of Education.

REFERENCES

[1] for example :Proc. of JCI Colloquim on Finite Element Analysis of RC Structures, JCI, Dec., 1984
[2] Collins, M.P. and Vecchio, F.J. :The Response of Reinforced Concrete to In-plane Shear and Normal Stresses, University of Toronto, March, 1982
[3] Maekawa, K. :Constitutive Law of Concrete based on the Elasto-Plastic and Fracture Theory, Proc. of JCI 2nd. Colloquim on Shear Analysis of RC Structures, Vol.JCI-C5, Oct., 1983, pp.1-8 (in Japanese).
[4] Yamada, K and Aoyagi, M. :Shear Transfer on the Cracked Surface, Proc. of JCI 2nd. Colloquim on Shear Analysis of RC Structures, Vol.JCI-C5, Oct., 1983, pp.19-28 (in Japanese).
[5] Miyahara, T., Kawakami, T. and Maekawa, K. :Nonlinear Behavior of Cracked Reinforced Concrete Plate Element Under Uniaxial Compression, Proc. of JSCE, No.378, Feb., 1987, pp.249-258, Concrete Library of JSCE No.11, June, 1988, pp.131-144.
[6] Tamai, S., Shima, H., Izumo, J. and Okamura, H. :Average Stress-Strain Relationship in Post Yield Range of Steel Bar in Concrete, Proc. of JSCE, No.378, Feb., 1987, pp.239-247, Concrete Library of JSCE No.11, June, 1988, pp.117-129.
[7] Okamura, H., Maekawa, K. and Sivasubramaniyam, S :Verification of Modeling

for Reinforced Concrete Finite Element, Finite Element Analysis of Reinforced Concrete Structures, Proc. of the Seminar ASCE, Aug., 1985, pp.528-543,
[8] Aoyagi, Y. and Yamada, K. :Strength and Deformation Characteristics of Reinforced Concrete Shell Elements Subjected to In-plane Forces, Proc. of JSCE, No.331, March, 1983, pp.167-190, Concrete Library International, No.4, Dec., 1984, pp.129-160
[9] Kupfer,H.B. and Gerstle, K.H. :Behavior of Concrete Under Biaxial Stresses, Proc. of ASCE, EM4, ASCE, Aug., 1973, pp.853-866
[10] Niwa, J., Maekawa, K. and Okamura, H. :Nonlinear Finite Element Analysis of Deep Beams, Final Report IABSE Colloqium, Delft, 1981
[11] Maekawa, K. and Okamura, H. :The Deformational Behavior and Constitutive Equation of Concrete Using the Elasto-Plastic and Fracture Model, Journal of Faculty of Engineering, the University of Tokyo (B) Vol. X X X Ⅶ, No.2, 1983
[12] Fukusi, T., Okazima, M. and Okamura, K. :Study on Prestressed Concrete Nuclear Containment Vessel, Proc. Annual Conv., AIJ, Sept., 1978, pp.1815-1816 (in Japanese).
[13] Gilbert, R.I. and Warner, R.F. :Tension Stiffening in Reinforced Concrete Slabs, Proc. of ASCE, ST12, Dec., 1978, pp.1885-1900
[14] CEB :Bulletin d'Information, No.117, 1977
[15] Morita, S. and Kaku, T. :Study on Bond Effect of Reinforced Concrete members by Tension Test, Cement Technology Annual Report, The Cement Association, No.18, 1964, pp.426-430 (in Japanese)
[16] Yoshikawa, H. and Tanabe, T. :An Analytical Study for Tension Stiffness of Reinforced Concrete Members on the Basis of Bond-Slip Mechanism, Proc. of JSCE, No.366, Feb., 1986, pp.93-102 (in Japanese)
[17] Milford, R.V. and Schnobrich, W.C. :Behavior of Reinforced Concrete Cooling Towers, University of Illinois at Urabana-Champaign, Illinois, May, 1984
[18] Vecchio, F.J. and Collins, M.P. :The Modified Compression-Field Theory for Reinforced Concrete Elements Subjected to Shear, ACI Journal, March-April, 1986, pp.219-231
[19] Kamisakoda, K., Maekawa, K. and Okamura, H. :Uniaxial Compression Strength of Concrete, Proc. of JCI 4th Conference, 1982, pp.177-180 (in Japanese)
[20] Cervenka, V. :Constitutive Model for Cracked Reinforced Concrete, ACI Journal, Nov-Dec., 1985, pp.877-882
[21] Fardis, N. and Buyukozturk, O. :Shear Stiffness of Concrete by Finite Elements, Proc. of ASCE, ST6, June, 1980, pp.1310-1327
[22] Fenwick, R.C. and Paulay, T. :Mechanisms of Shear Resistance of Concrete Beams, Proc. of ASCE, ST10, Oct., 1968, pp.2325-2349
[23] Walraven, J.C. :Fundamental Analysis of Aggregate Interlock, Proc., ASCE, Vol.107, ST11, Nov., 1981
[24] Shioya, T. and Kawasaki, H. :A study on Size Effect in Shear Strength of Reinforced Concrete Beams, Proc. of JCI Colloquim on Finite Element Analysis of RC Structures, JCI, Dec., 1984, pp.151-158 (in Japanese)

APPENDIX I

By considering the equilibrium-of-force of the free body with regard to x and y directions, eq.(1-1) and eq.(1-2) can be introduced (see Fig.1.1). The equilibrium of forces with regard to x and y directions are given by eq.(1-1) and eq.(1-2)

$$\sigma_{sx}A_{sx}\cos\alpha - \sigma_{sy}A_{sy}\sin\alpha - \tau ABt\sin\theta + \sigma_{c}ABt\cos\theta = \sigma_{x}BCt + \tau_{xy}ACt \quad (1\text{-}1)$$

$$\sigma_{sx}A_{sx}\sin\alpha + \sigma_{sy}A_{sy}\cos\alpha + \tau ABt\cos\theta + \sigma_{c}ABt\sin\theta = \sigma_{y}ACt + \tau_{xy}BCt \quad (1\text{-}2)$$

The reinforcement ratio being defined by the rate of the cross-sectional area of steel to the area of the RC panel element crossing in the direction orthogonal to the steel bar axis, eq.(1-3) and eq.(1-4) can be introduced as follows.

$$p_x = A_{sx}/BDt = A_{sx}/\{ABt\cos(\theta-\alpha)\} \quad (1\text{-}3)$$

$$p_y = A_{sy}/ADt = A_{sx}/\{ABt\sin(\theta-\alpha)\} \quad (1\text{-}4)$$

From geometrical condition, eq.(1-5) can be given by;

$$\sin\theta = AC/AB$$
$$\cos\theta = BC/AB \quad (1\text{-}5)$$

Eq.(1-1) and eq.(1-2) being rewritten by using eq.(1-3), eq.(1-4) and eq.(1-5), eq.(1-6) and eq.(1-7) can be introduced.

$$p_x\sigma_{sx}\cos(\theta-\alpha)\cos\alpha - p_y\sigma_{sy}\sin(\theta-\alpha)\sin\alpha = (\sigma_x-\sigma_c)\cos\theta + (\tau_{xy}+\tau)\sin\theta \quad (1\text{-}6)$$

$$p_x\sigma_{sx}\cos(\theta-\alpha)\sin\alpha - p_y\sigma_{sy}\sin(\theta-\alpha)\cos\alpha = (\sigma_y-\sigma_c)\sin\theta + (\tau_{xy}-\tau)\cos\theta \quad (1\text{-}7)$$

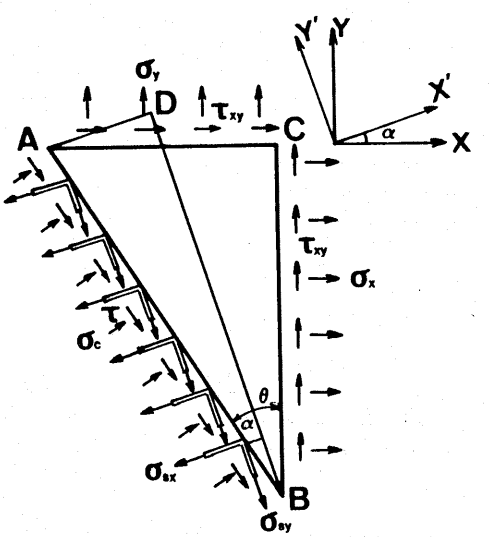

Fig. 1.1 Stresses act on the free body

Eq.(1-6) and eq.(1-7) being solved regarding to $p_x\sigma_{sx}$ and $p_y\sigma_{sy}$, eq.(1-8) and eq.(1-9) are obtained.

$$p_x\sigma_{sx}=\frac{\cos\alpha}{\cos(\theta-\alpha)}\{(\sigma_x-\sigma_c)\cos\theta+(\tau_{xy}+\tau)\sin\theta\}$$

$$+\frac{\sin\alpha}{\cos(\theta-\alpha)}\{(\sigma_y-\sigma_c)\sin\theta+(\tau_{xy}-\tau)\cos\theta\} \quad (1\text{-}8)$$

$$p_y\sigma_{sy}=-\frac{\sin\alpha}{\sin(\theta-\alpha)}\{(\sigma_x-\sigma_c)\cos\theta+(\tau_{xy}+\tau)\sin\theta\}$$

$$+\frac{\cos\alpha}{\sin(\theta-\alpha)}\{(\sigma_y-\sigma_c)\sin\theta+(\tau_{xy}-\tau)\cos\theta\} \quad (1\text{-}9)$$

σ_{sx} and σ_{sy} obtained by eq.(1-8) and eq.(1-9) are the steel stresses at the cracked face.

APPENDIX II

Assumed that the stress distribution of steel after yielding between cracks is expressed by a cosine function as shown in Fig.2-1, the steel stress can be given by eq.(2-1).

$$\sigma_s=-A\cos\pi x+\overline{\sigma}_s \quad (2\text{-}1)$$

Further, the mean steel strain is expressed by eq.(2-2), using eq.(2-1).

$$\overline{\varepsilon}_s=\int_0^{x_1}(\sigma_s/E_s)dx+\int_{x_1}^{1}\{\varepsilon_{sh}+(\sigma_s-f_y)/E_{sh}\}dx$$

$$=\{\frac{x_1}{E_s}+\frac{(1-x_1)}{E_{sh}}\}\overline{\sigma}_s+\varepsilon_{sh}(1-x_1)-\frac{f_y}{E_{sh}}(1-x_1)+(\frac{1}{E_{sh}}-\frac{1}{E_s})\sin\pi x_1 \quad (2\text{-}2)$$

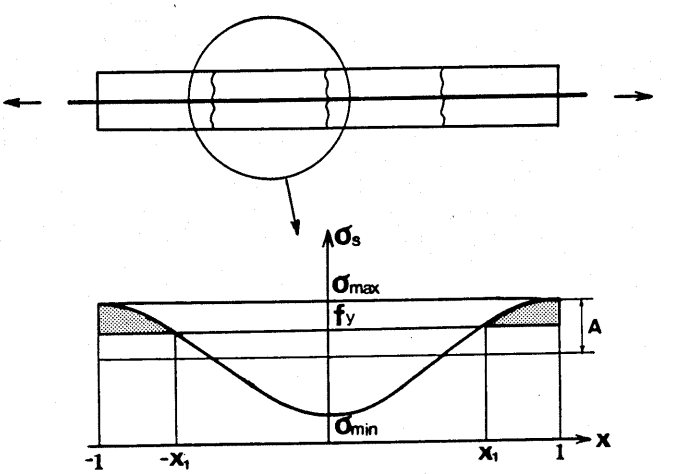

Fig.2-1 Modelling of the steel stress distribution after yielding between cracks

x_1 indicates the normalized length of elastic parts along the steel bar and can be obtained by substituting f_y for σ_s in eq.(2-1).

$$x_1=\frac{1}{\pi}\cos^{-1}\left(\frac{\overline{\sigma}_s-f_y}{A}\right) \tag{2-3}$$

Eq.(2-2) being solved regarding to the steel stress; σ_s, eq.(2-4) can be introduced.

$$\overline{\sigma}_s=K_1(\overline{\varepsilon}_s-K_2) \tag{2-4}$$

where, $K_1=1/\left\{\frac{x_1}{E_s}+\frac{(1-x_1)}{E_{sh}}\right\}$, $K_2=\varepsilon_{sh}(1-x_1)-\frac{f_y}{E_{sh}}(1-x_1)+\left(\frac{1}{E_{sh}}-\frac{1}{E_s}\right)\sin\pi x_1$

Steel stress after yielding is obtained by using eq.(2-3) and eq.(2-4). In this analysis, steel stress after yielding has been obtained by repeating calculation with eq.(2-3) and eq.(2-4), assuming the stress amplitude of steel A expressed by eq.(2-5)

$$A=A_0(\varepsilon_{s0}/\varepsilon_s)^c \tag{2-5}$$

Eq.(2-5) indicates that the lowering stress amplitude of steel is assumed be approximately equal to the lowering of tension stiffening.